www.revistageintec.net
ISSN: 2237-0722
revista GEINTEC Gestão, Inovação e Tecnologias

Fatigue and Stress Analysis of a Load Carrying Car Chassis with Reinforced Joint Using Finite Element Method

Arash Babamiri[1]; Shaghayegh Hadian[2]; Greg Wheatley[3*]

[1]Department of Engineering, Graduate Student of Mechanical Engineering, University of Kurdistan, Kurdistan, Iran.

[1]Arash.babamiri71@gmail.com

[2]Department of Engineering, Graduate Student of Mechanical Engineering, Ferdowsi University, Mashhad, Iran.

[2]shaghayeghsh2.mr11@yahoo.com

[3*]Senior Lecturer of Mechanical Engineering, College of Science & Engineering, James Cook University, Townsville, Australia.

[3*]Greg.Wheatley@jcu.edu.au

Abstract

In this article, a case study of a load-carrying vehicle chassis with various loading conditions in six maneuvers has been conducted. These maneuvers include acceleration and deceleration in a loaded and un-loaded situation, drops, pothole, turn, and sinusoidal obstacles. Finite element analysis has been implemented in order to calculate stress distribution and fatigue life. Stress analysis indicated that the joints stiffness is higher where the auxiliary profiles were utilized. However, this procedure is cumbersome and auxiliary plates would be a more efficient strategy. The effects of using auxiliary plates have been investigated in the fatigue and stress distribution of the aforementioned chassis. The analysis revealed that the 300 mm drop has the maximum tension and accordingly embodies the shortest fatigue life. Furthermore, for welding joints, three different strategies for geometry configuration including welding bead, reinforcing plates, and extra auxiliary profiles under the welded joints were assumed.

Key-words: Car Chassis, Suspension System, Fatigue Life, welding Joints, Finite Element Method.

1. Introduction

Automobiles are an inevitable part of the modern era and their popularity has encouraged engineers to improve their safety and comfort (Podkowski et al., 2019; Ren et al., 2017; Sharma et al., 2021). These goals are not out of reach with an endurable car chassis that is designed properly. A suitable vehicle chassis design includes stress, fatigue, and vibration analysis (Bhatnagar et al., 2018;

N et al., 2018). With the increased usage of numerical simulation over the past few decades in the car industry (Ablat & Qattawi, 2017; Khatoon & Kim, 2020), car manufacturers and researchers are able to simulate various maneuvers in which the chassis experience high tension (Str et al., 2019). Numerical simulation can save considerable time and expenditures (Oanta et al., 2020; Y. Wang et al., 2019) and the produced results can lead to designing a more efficient chassis. Designing an effective chassis required meticulous attention to welds, suspension system, and structure design that will be discussed in detail in the following.

The chassis efficiency can be limited by its welded component since welding may result in degradation to mechanical property (P. Wang et al., 2018). The importance of welding in fatigue life has encouraged researchers to focus on this subject. (Fricke, 2003) reviewed how to develop fatigue analysis in welded joints over the last 10-15 years. (MENEGHETTI, 2008) proposed the application of the peak stress method in estimating the fatigue of welded pipe joints under the influence of the first loading mode. They showed that using this method is suitable for estimating the fatigue life of such connections. (Chattopadhyay et al., 2011) presented general rules for meshing in order to obtain flexural and structural stresses and finally calculated the initial fatigue crack life with the help of peak stress at the welding foot. (Kim et al., 2015) presented a new numerical method for calculating hot spot stress that is less sensitive to mesh. They used the method of work and equivalent force to calculate the welding foot stress measured at specific intervals. Finally, they showed that the use of quadratic elements with reduced integrals has the least error.

The suspension system has a deep correlation with car chassis since they are linked together via control arms. Therefore, an effective chassis cannot be designed without consideration of the suspension system. Accordingly, researchers have been convinced to develop a high-performance double wishbone which is an important part of a suspension (Sankar et al., 2018). Prior to them, (Balaji et al., 2017) optimized the double-wishbone suspension system based on the road profile of India via Finite Element Analysis (FEA). Likewise, Balaji et al., (Zaidie et al., 2017) utilized the Finite Element Method (FEM) to analyze and design a new front suspension system that performed better in braking, cornering, and bumping.

Finally, the chassis structure should be evaluated from the stress and fatigue perspective. Hence, (Gorash et al., 2015) investigated the effect of fatigue data and finite element states on the accuracy of estimating the remaining life of a sample under repetitive fatigue conditions. To determine the failure location and estimate the fatigue life, the Volvo method is implemented and the effect of parameters such as thickness, bending, and average stress according to BS7608 was considered. In the same year, (Paraforos et al., 2016) investigated the effect of roughness on the fatigue life of agricultural machines.

They used the Palmgren-Miner law to estimate life. (Deulgaonkar, 2019), designed and analyzed both stress and vibration of a transport utility vehicle. He investigated structure deflection, modal analysis, and the importance of meshing. Another comprehensive study was done by (Abry et al., 2018), in which they evaluated finite element model preparation for stress, fatigue, and welding of a heavy vehicle chassis frame. Their results were validated with 10 years of operating experience. Chassis of the specific vehicles such as All-Terrain Vehicle (ATV) (Kumar et al., 2020), Tractor Trolley (Deulgaonkar, 2019), electric car (Tsirogiannis et al., 2019), and formula student car (Hazimi et al., 2018; Mohamad et al., 2017; Wongchai, 2020) have been assessed by other researchers.

According to the aforementioned literature review, although stress and fatigue analysis have been considered for cars' chassis, joints connections in the main frame are a huge void in chassis design. In this paper, this gap will be bridged by considering three strategies for welding joints. To determine the feasibility of these strategies, the load-carrying car chassis is going to experience different road profiles. Consequently, stress analysis can be a key factor for distinguishing the efficacious strategy. After choosing the best strategy, fatigue life prediction will be calculated for the chassis with its new weld condition.

2. Materials and Methods

A. Geometry

The main frame consists of a profile with dimensions of 170 × 70 × 3.5 mm; however, a coned shape profile was used at the end of each branch. Squire shape tube and C shape profile have been utilized for supporter and connector, respectively. Elastic modulus and Poisson's ratio for all of the steel parts are 200 MPa and 0.3 respectively. For the suspension parts, two groups of springs have been implemented. Stiffness of the first group, front wheels, is 240741 N/m and the stiffness of second group springs are equal to 448247 N/m.

Additionally, three different geometry have been considered for the profile connection:

- Modeling of welding with a 2.5 mm bead height (Fig. 2a). In this case, it is assumed that the two profiles are butt welded.
- Creating a distance of 15 mm between the two profiles at the joint and using reinforcement plates with 6 mm thickness and 40 mm width. The empty space between the two joints is filled by welding. This strategy, which is the novelty of the current study, will simulate lap joint for the chassis profile (Fig. 2b).

- Creating a distance of 15 mm between the two profiles at the joint and using a 6 mm reinforcing profile that perfectly matches the geometry of the joint and then filling the empty space between the two joints by welding (Fig. 2c).

Figure 1 - Isometric, Top, and Side View of the Chassis

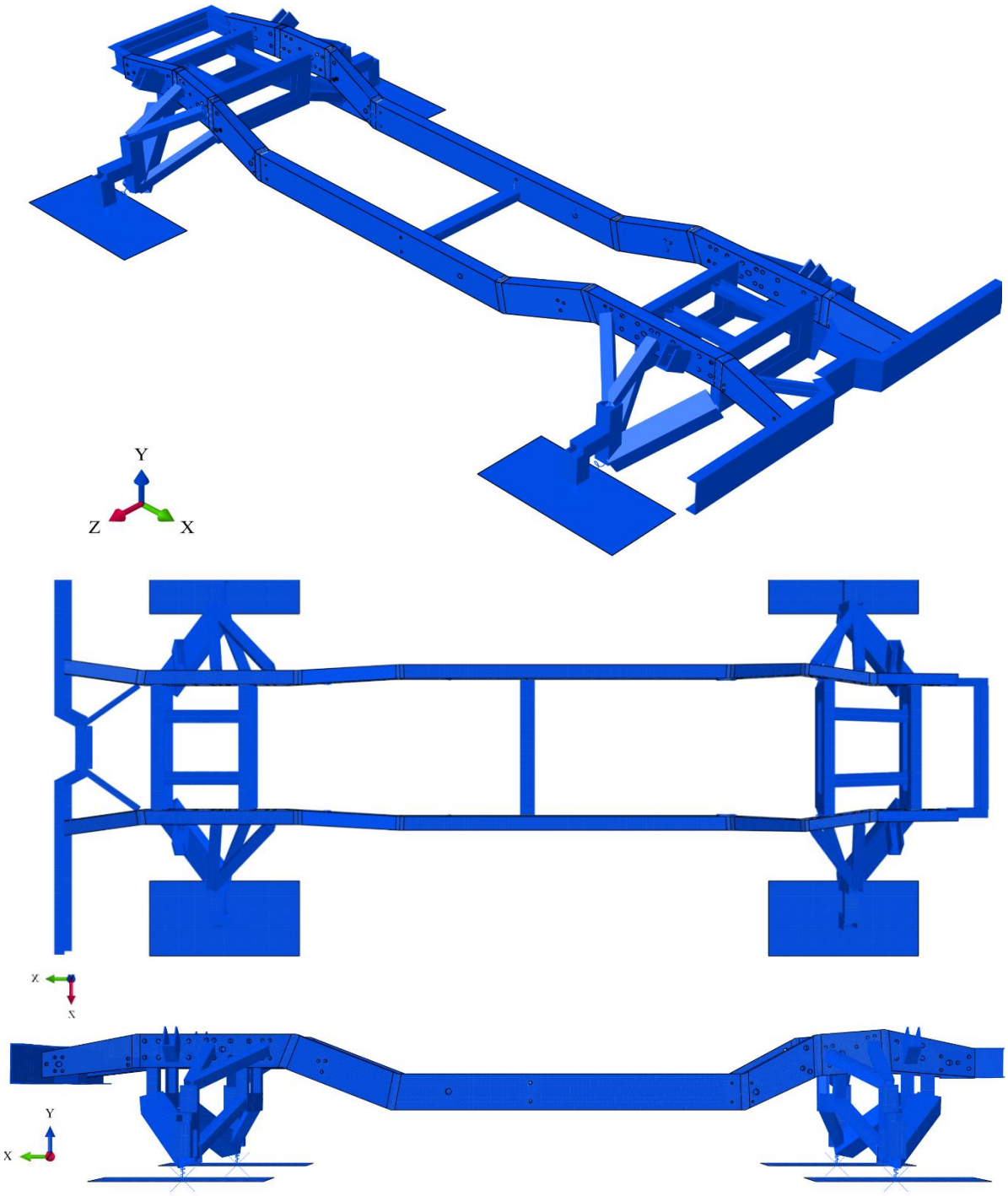

Figure 2 - Isometric View of different Strategies for Connection Welding. a) Weld Bead. b) Reinforcement Plate. c) Extra Auxiliary Profiles

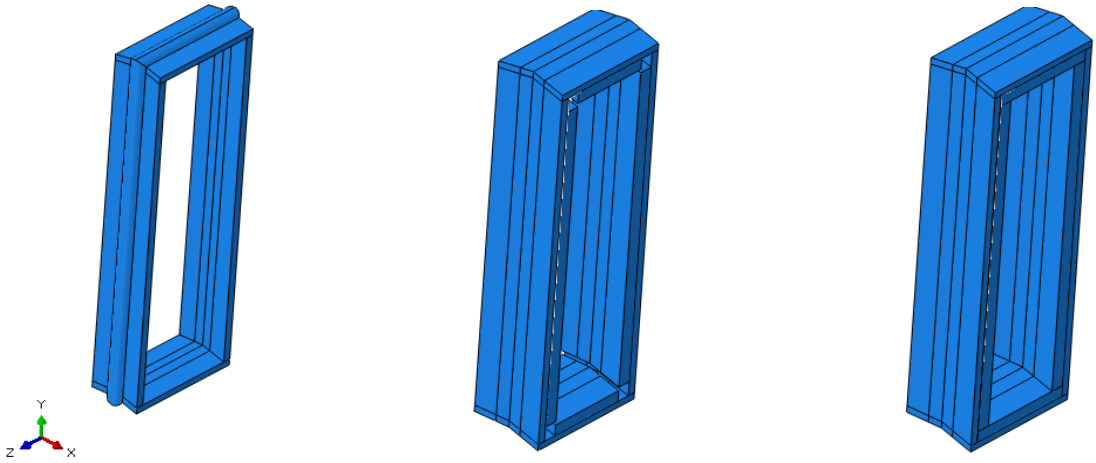

a b c

B. Finite Element Analysis

The chassis consists of three major parts with different priorities and importance in stress distribution. Connec-tion parts in which there is stress concentration due to its weld geometry, the main frame which is more uniform, and links, also known as the suspension system, that connect the main frame to the wheels. To simulate these three parts solid (C3D8R), shell (S3), and beam (B31) elements have been considered (Fig. 3). These divisions can lower the number of the element dramati-cally and accordingly reduce the simulation time.

Figure 3 - Utilized Elements in the Simulation

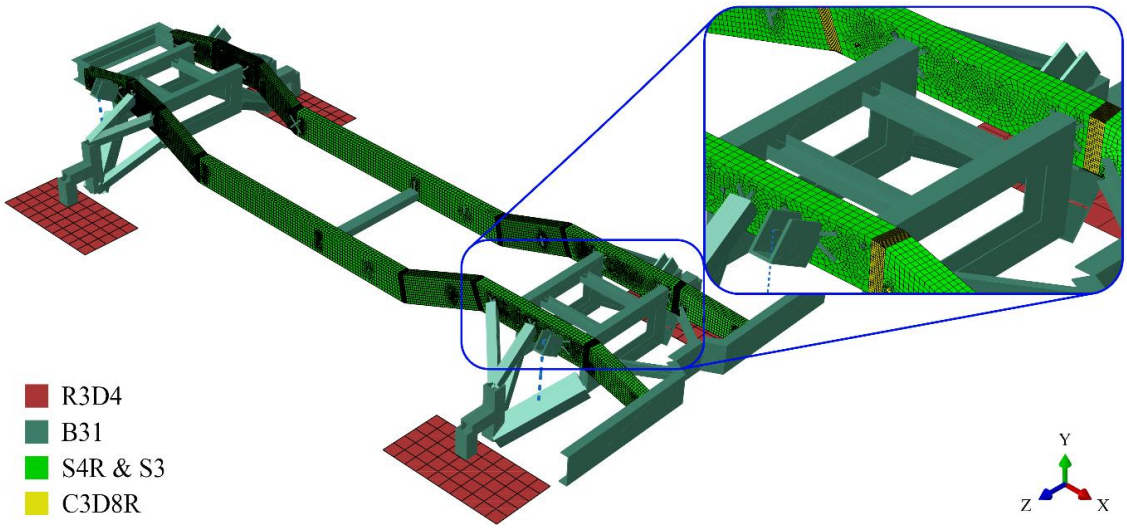

Loading and Weight

The whole chassis has been divided into three section and some points that represent the mass of the car have been assigned to each section as follow: I) Front with 3 points II) Middle with 4 points and III) Rear with 3 points. All these points are coupled to the main frame in order to transfer the mass effect to the chassis.

Total car weight has been divided into 10 points in order to have a more uniformly distributed mass. However, the division must meet the following requisition:

- The total weight of the 10 points must be equal to the total weight of the car.
- Central gravity of the 10 points must coincide with the CG of the car.
- Moment inertia of these points must be equal to the moment inertia of the car.

The aforementioned requirements bear the following equations:

$$3m_R + 4m_M + 3m_F = M \quad (1)$$

$$3m_R l + 18m_M l + 24m_F l = ML_G \quad (2)$$

$$m_R[L_G^2 + (L_G - l)^2 + (L_G - 2l)^2] + m_M[(L_G - 3l)^2 + (L_G - 4l)^2 + (L_G - 5l)^2 + (L_G - 6l)^2] + m_{MF}[(L_G - 7l)^2 + (L_G - 8l)^2 + (L_G - 9l)^2] = I_{ZZ} \quad (3)$$

In which m_R, m_M, and m_F are mass of each point in the rear, middle, and front of the car. M represents the mass of the car and L_G is the distance of the CG from the rear bumper and I_{zz} is the second-moment inertia of the car. By considering the l= 508 mm, L_G= 2090 mm, and car width of 2000 mm the outcome of the equation can be summarized in Table 1.

Table 1 - Weight and Second-moment Inertia of the Car's Chassis

	Loaded car (5000 Kg)	**Empty car (3500 Kg)**
m_R **(Kg)**	590	413
m_M **(Kg)**	505	353
m_F **(Kg)**	405	283
I_{xxR} **(Kg.m^2)**	195	136
I_{xxM} **(Kg.m^2)**	185	129
I_{xxF} **(Kg.m^2)**	135	94

The suspension system has been modeled as axial connectors and the mechanical property for the springs are as shown in Table 2. In this table δ_0, L_{comp}, and K are Initial pre-compression, compressed length, and stiffness of the springs, respectively.

Table 2 - Initial Pre-compression, Compressed Length, and Stiffness of the Front and Rear Springs

	δ_0 (m)	L_{comp} (m)	K (N/m)
Front	0.042	0.201	240741
Rear	0.048	0.264	448247

Maneuvers and Boundary Condition

Six major maneuvers of a car have been investigated in this article. Table 3 represents a summary of these maneuvers. It has been assumed that in the loaded situation the car has an acceleration of 3 m/s^2 and in the empty case this acceleration increase to 5 m/s^2. In deceleration, the direction of the acceleration will change in the opposite direction and the magnitude will remain constant.

Table 3 - Maneuvers Implemented on the Chassis and their Characteristics

	acceleration	**deceleration**	**pothole**	**Drop**	**Sinusoidal obstacle**	**turning**
Case 1	Loaded	Loaded	300mm deep	100 mm	Different phase for each side	Specific radius and velocity
Case 2	Empty	Empty	×	300 mm	×	×

In the pothole maneuver, the car's velocity is assumed to be 0.762 m/s and the configuration of the pit is illustrated in Fig. 4. In this situation, the rigid plane will move a profile similar to Fig. 4. It is also worth mentioning, according to the length of the car, rear wheels will experience the same pothole profile with a five-second delay.

Figure 4 - Displacement Induced on the Front and Rear Wheels for the Pothole Maneuver

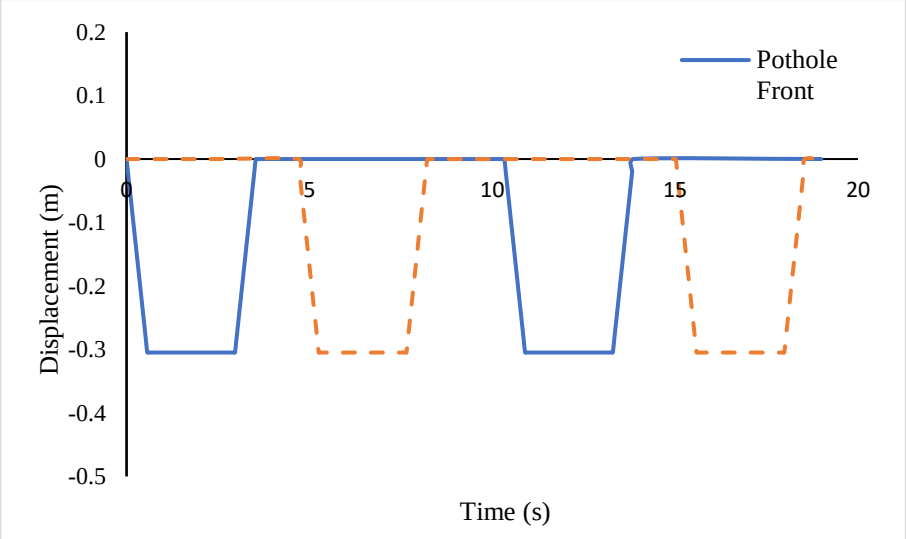

Received: 28.05.2021 – Accepted: 25.06.2021

In the drop condition, it has been supposed the chassis is in the effect of gravity and will be released from a particular height. In this case, rigid planes are fixed to simulate a hard ground for the wheels. In another maneuver, it is assumed that the chassis passes a sinusoidal obstacle. However, the right and left side profiles have different phases (see Fig. 5). Rear wheels will experience a similar profile according to the logic described for the pothole.

Figure 5 - The Sinusoidal Obstacle for the Right and Left Wheels

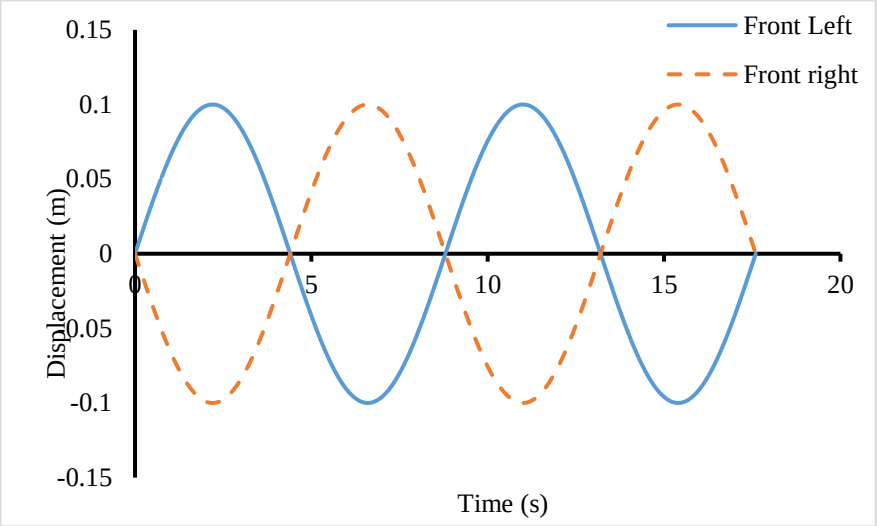

For the final maneuver, which is turning, the car turns a 95 m curve path. According to (James L. Meriam, L. G. Kraige, 2015), passing a curved path will exert a radial force on the chassis (Eq. 4).

$$F = m\frac{V^2}{r} \qquad (4)$$

In which m, V, and r are mass, velocity, and curvature radios, respectively. The following diagram (Fig. 6) clearly illustrates the procedure of doing the analysis in this article. Although ABAQUS is capable of performing a variety of analyses; in this article, the stress distribution is the aim of using this software.

Figure 6 - Procedure of performing the analysis.

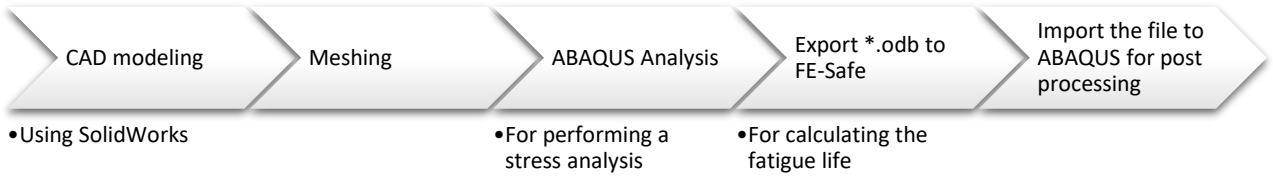

C. Fatigue Life Evaluation

Since the chassis is usually dealing with dynamic forces during the service, fatigue analysis is another important criterion that should be evaluated. In order to estimate the fatigue life of the chassis, FE-Safe is implemented. By determining the stress distribution in the chassis, the odb file must export to the software. Afterward, the stress ratio will be entered by the user that allows stress exerts to the component repetitively. Finally, these results can be imported to ABAQUS for post-processing.

3. Results

In the first stage of the analysis, a comparison between the three mentioned strategies has been done. For this comparison, a hypothetical maneuver is defined to reveal the best strategy for the whole chassis. In this hypothetical maneuver, the left side of the profile is completely fixed and the right side is 950 Nm and the vertical upward force is 1000 N. To apply these forces a rigid plate has been used. (Fig. 7)

Table 4 - Maximum Von Mises Stress for a different strategy in the Unreal Maneuver

Strategy	**Maximum Von Mises stress (Mpa)**
Joint with simulated bead geometry	83.4
Joint with auxiliary plates	56.2
Joint with auxiliary profile	48

Figure 7 - Hypothesis Maneuver for a Part of the Chassis

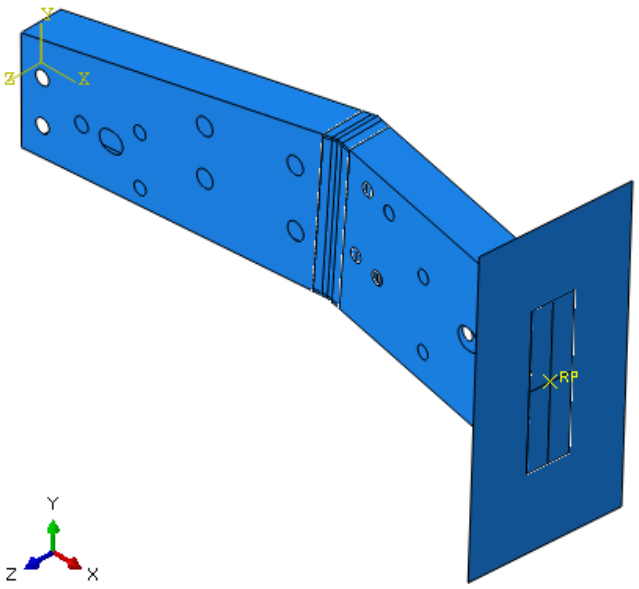

Table 4 summarizes the results of this hypothetical maneuver. These results revealed that using an auxiliary plate reduces maximum Von Mises stress by 14%, and the auxiliary profile is roughly 43% more effective than the joint without reinforcement. In addition to the supposed condition, the results have been verified for the acceleration maneuver.

Table 5 - Verifying the Best Strategy for the joints in the Acceleration Maneuver

Maneuver	**Strategy**	**Maximum Von Mises stress (Mpa)**
Empty acceleration	Joints with an auxiliary plate	200.6
	Joints with auxiliary profile	141.2

According to Table 4 and Table 5, using the reinforcement profiles is more effective in reducing the maximum Von Mises stress than other strategies. However, it is not cost-effective due to the need to build a mold. Therefore, it is recommended to use reinforcement plates for the main chassis.

In order to alleviate the mesh dependency, suitable mesh size for the first maneuver, empty (unloaded) acceleration, has been determined by trial and error approach. For a supposed path, which is far from stress concentration points, the best element size has been evaluated according to Figure 7. Since the change percentage for the two last analyses is 4.07, 44204 element is a fine mesh size, and the rest of the analyses have been conducted based on this element size.

Figure 7 - Mesh Convergence Analysis for the Mentioned Chassis

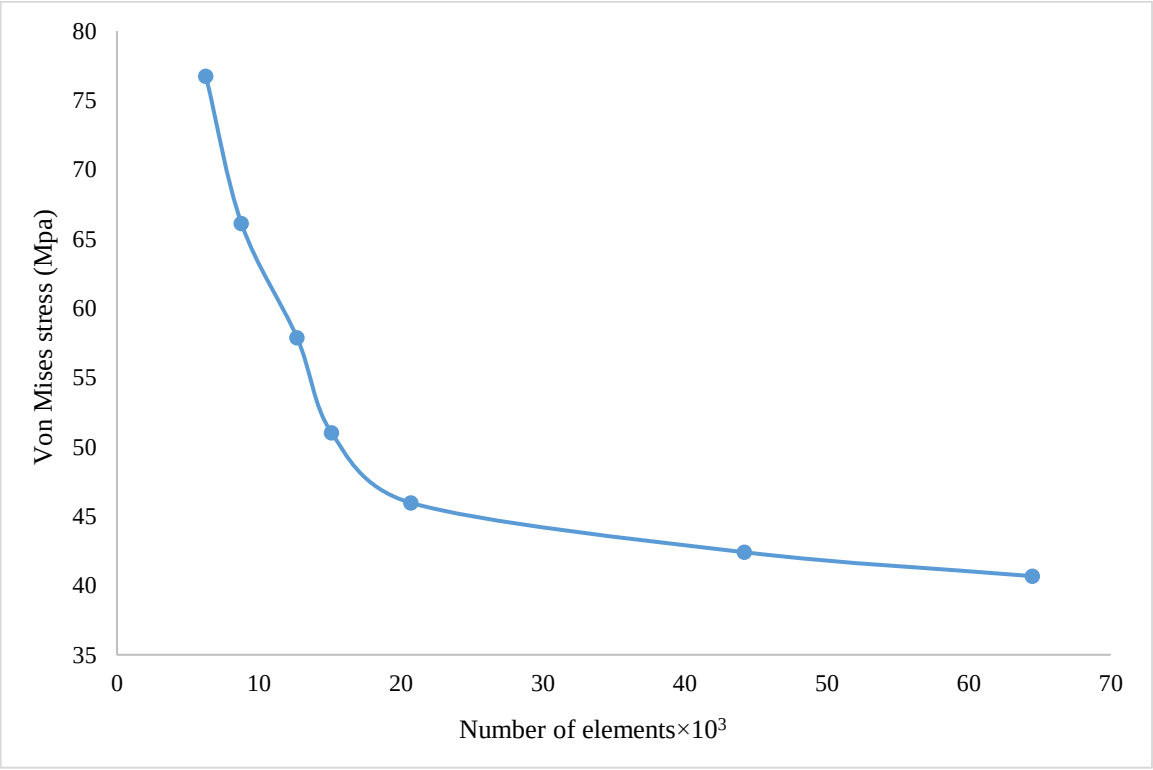

In loaded and empty acceleration maneuvers, the maximum stress is 168.1 MPa and 200.6 MPa respectively (Figure 8 a,b). For full and empty deceleration maneuvers, the results of stress analysis are in accordance with Table 6, which are presented in Figure 9 a and b, respectively.

Table 6 - Maximum Von Mises Stress for the Full and Empty Deceleration Maneuvers

	deceleration	**Maximum Von Mises stress (Mpa)**
Case 1	Loaded	207.8
Case 2	Empty	215.2

Figure 8 - Stress Analysis for the Acceleration Maneuver for a) Loaded Condition and b) Empty Situation

(a)

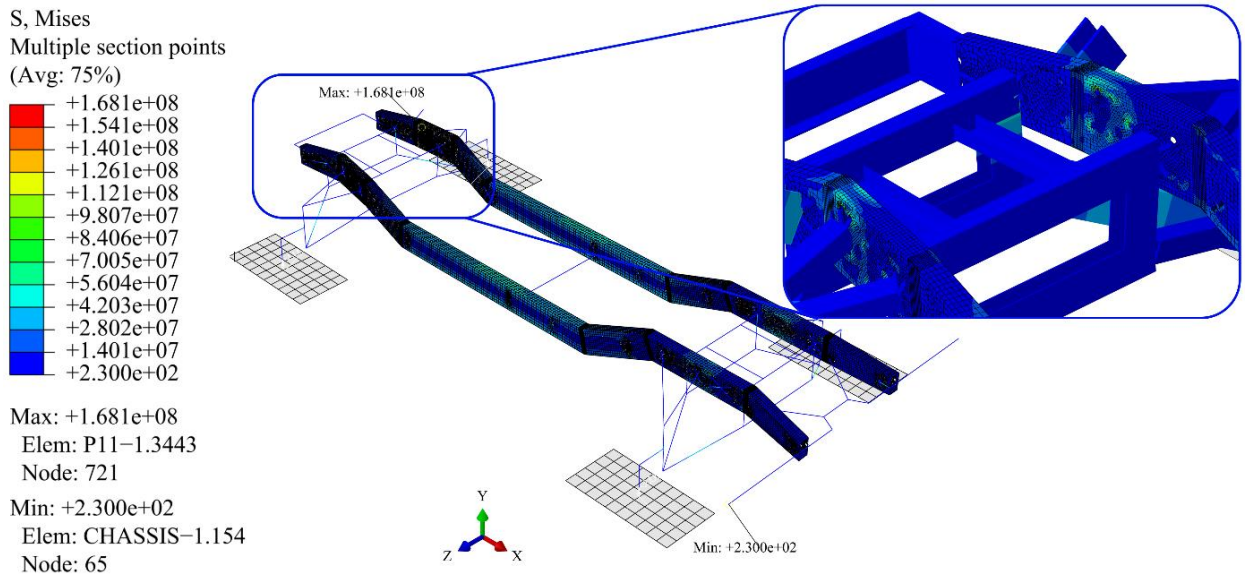

(b)

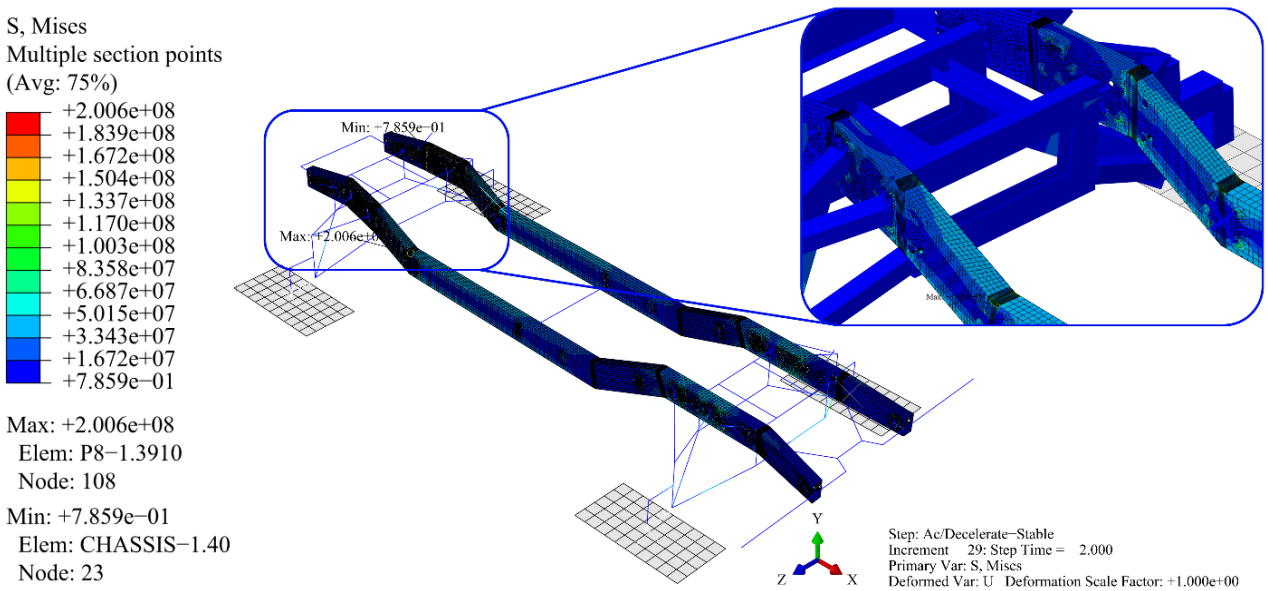

Received: 28.05.2021 – Accepted: 25.06.2021

Although in the loaded condition the chassis experience higher weight, the maximum stress in the chassis is lower. Since the chassis is for a pickup truck, adding extra load will result in more uniform weight distribution and the exerted load creates a balance between the front and rear parts of the chassis. Therefore, joints will experience lower stress.

Figure 9 - Effect of the Deceleration Maneuver for a) Loaded Condition and b) Empty Situation

(a)

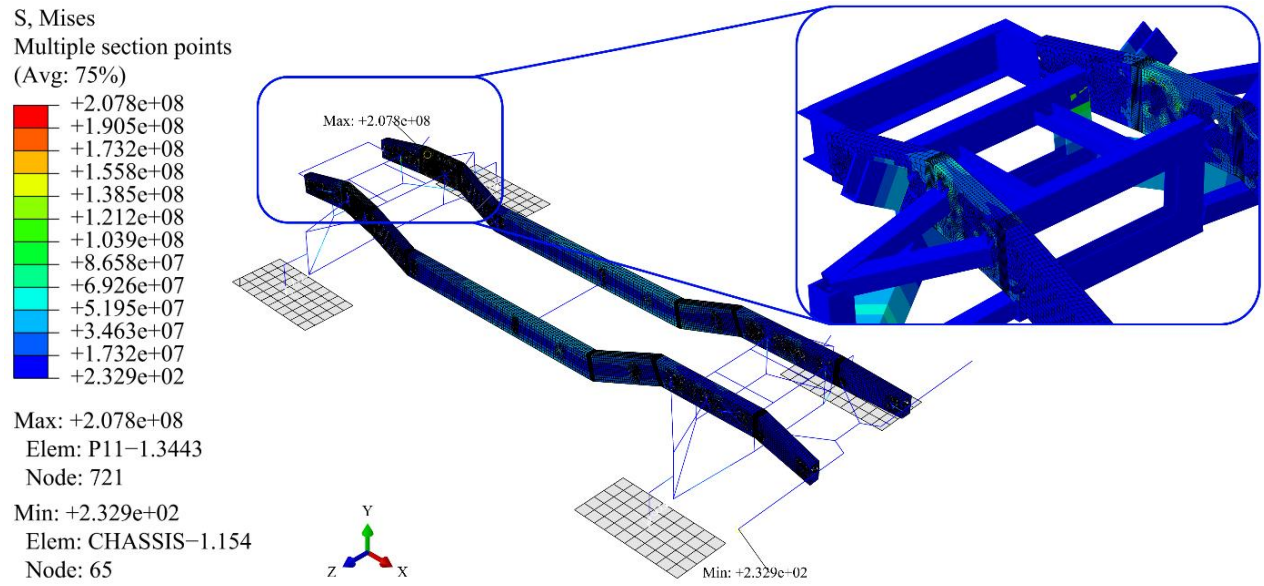

(b)

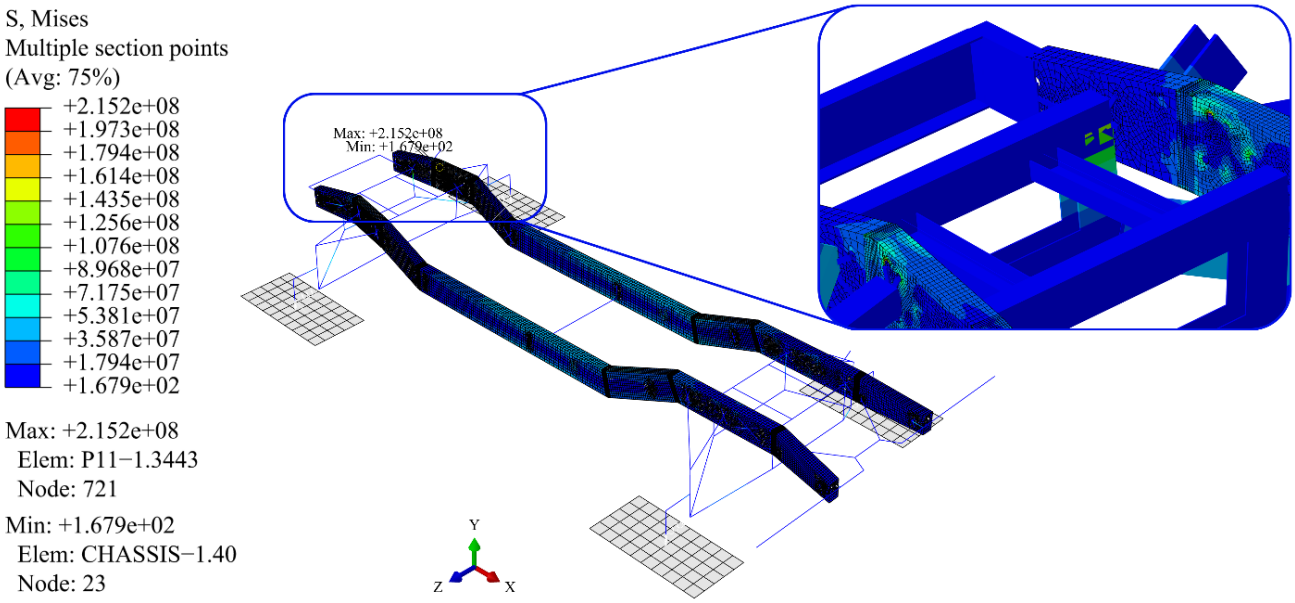

According to the similarity between acceleration and deceleration, the same results will happen for the loaded and empty cars. Therefore, higher stress will occur in the empty case in comparison to the full situation.

Figure 10 - Von Mises Stress for the Drop Maneuver from a) 100 mm and b) 300 mm

(a)

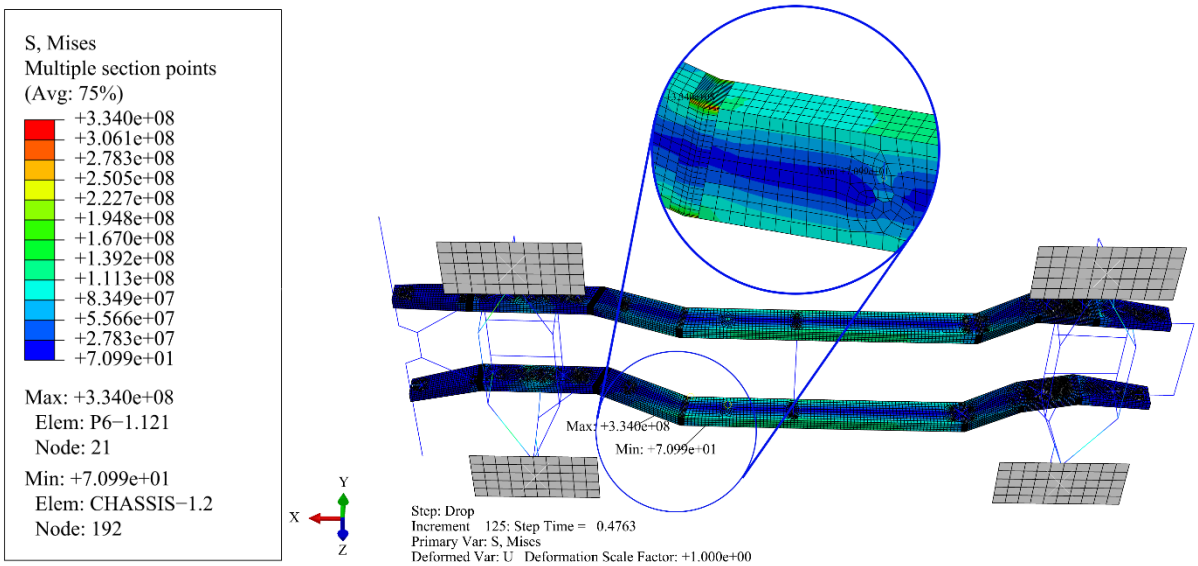

(b)

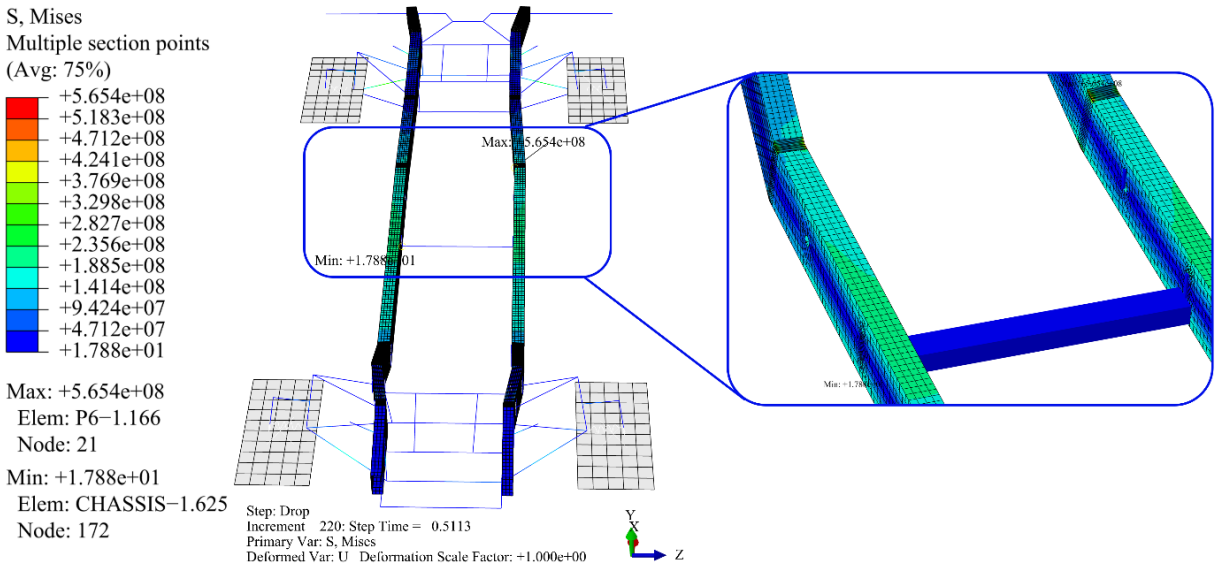

In this maneuver, the chassis will release from a specific height, and due to geometry characteristics, front wheels will touch the ground (rigid planes) earlier. As a result, the chassis will experience a bending situation. Due to the features of the bending, higher stress will happen in the

middle main beam. However, due to the stress concentration of the joints, this higher stress will shift towards joints.

In addition, it is worth mentioning that the upper left side of the chassis has slightly lower stress than the right side of the chassis, which has experienced the highest stress. This result has been derived according to the symmetrical properties of the geometry.

Figure 11 - Stress Analysis of the Chassis While Passing a Pothole

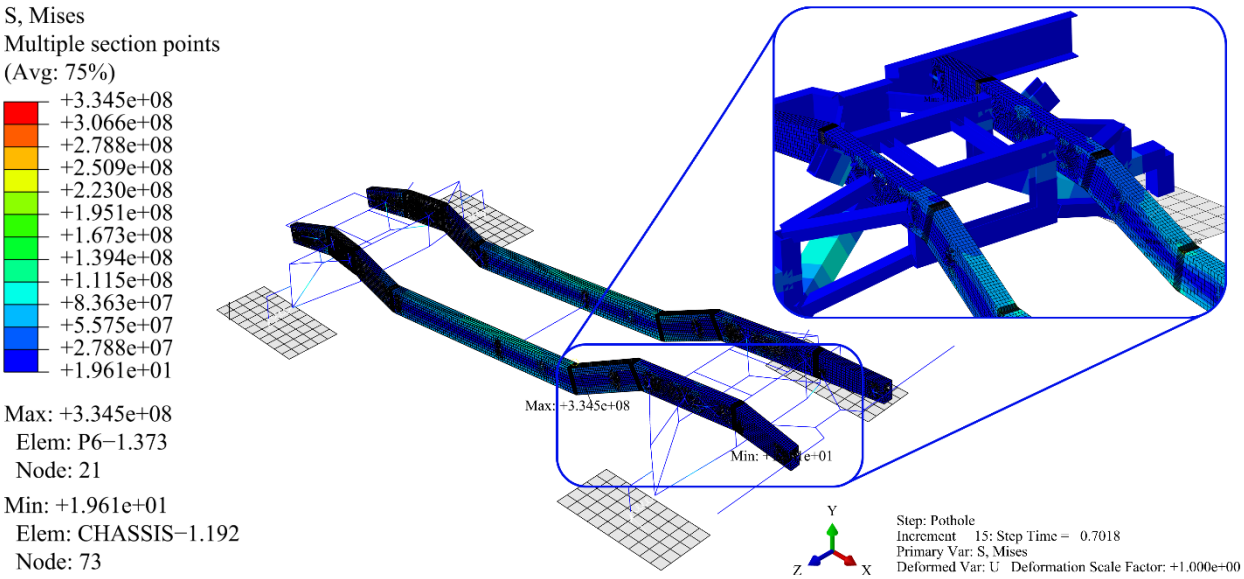

Figure 12 - Stress Analysis in the Sinusoidal Maneuver for the Chassis

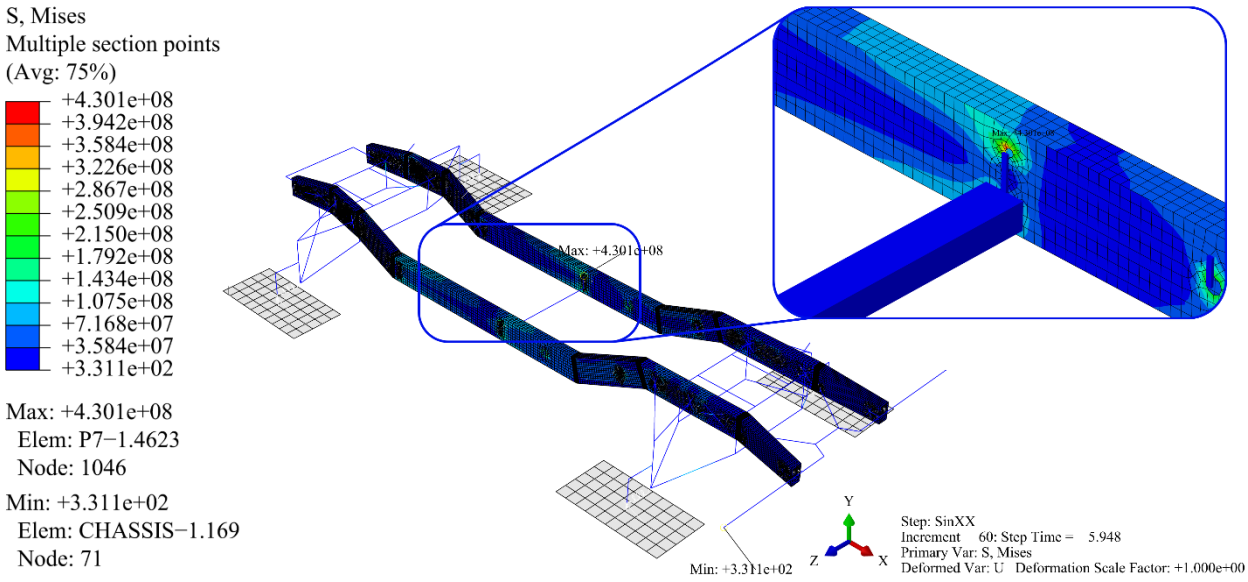

Due to the nature of the pothole and sinusoidal, the results for both maneuvers are similar to each other, in which the maximum Von Mises stress occurs in the central beam of the chassis. However, FEM analysis revealed that maximum stress for pothole and sinusoidal maneuvers are 334.5 MPa and 430.1 MPa, respectively. Since the chassis experiences torsion in sinusoidal maneuvers, the chassis will experience greater stress. An explanation for torsion is that right and left sides of the chassis experiences two different road profiles. While the right front wheel is at the top of the sinusoidal wave, the left front wheel is at the bottom of the wave at the same time.

Figure 13 - Stress Analysis for Chassis in Turning

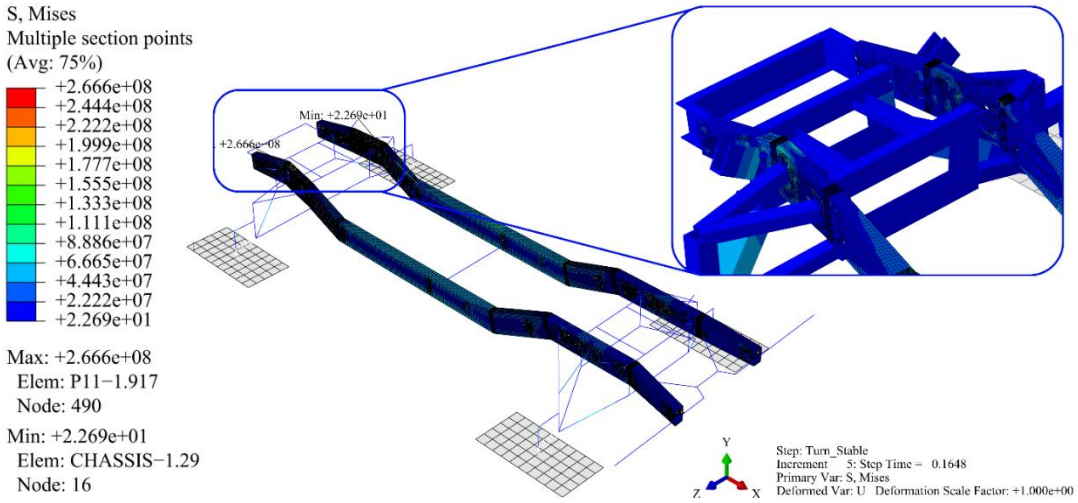

Fig. 14 represents stress distribution in the chassis while the car is passing a curved path. Since the right side of the chassis must pass a bigger curvature radius, due to the continuity of the chassis, lower stress will occur on this side. Moreover, a summary of maximum Von Mises stress for the drop, pothole, Sinusoidal obstacle, and turning maneuvers is presented in Table 7.

Table 7 - Maximum Von Mises Stress for the Drops, Pothole, Sinusoidal Obstacle, and Turning Maneuvers

Maneuver		**Maximum Von Mises stress (Mpa)**
Drop	**100 mm**	334
	300 mm	565
Pothole		334.5
Sinusoidal obstacle		430.1
Turning		266.6

In the following, the fatigue life of the chassis for all maneuver is evaluated by implementing the commercial FE-Safe software. The stress ratio is zero that is also known as the zero-to-tension condition and the S-N curve approach has been speculated.

The summary of fatigue life for all of the maneuver is presented in Table 8. As it is shown, the full acceleration maneuver is the safest move for the chassis with the highest fatigue life cycle and the 300 mm drop has the lowest fatigue life. According to stress analysis, these outcomes were predictable.

Table 8 - The Fatigue Life of the Chassis due to the Repetitive Maneuvers

	Empty acceleration	**Full acceleration**	**Empty deceleration**	**Full deceleration**	**pothole**	**Drop 100 mm**	**Drop 300 mm**	**Sinusoidal obstacle**
Fatigue life (cycle)	661000	1370000	448000	481000	105000	81000	25000	109000

Figure 14 - Fatigue Life Contour for all Maneuver. a) Empty Acceleration b) Full Acceleration c) Empty Deceleration d) Full Deceleration e) 100mm Drop f) 300mm Drop g) Sinusoidal h) Pothole

(a)

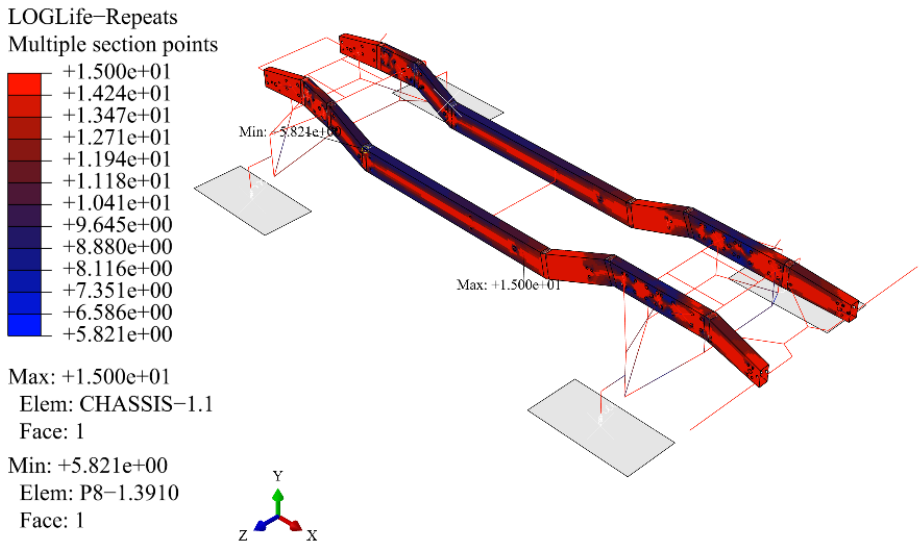

(b)

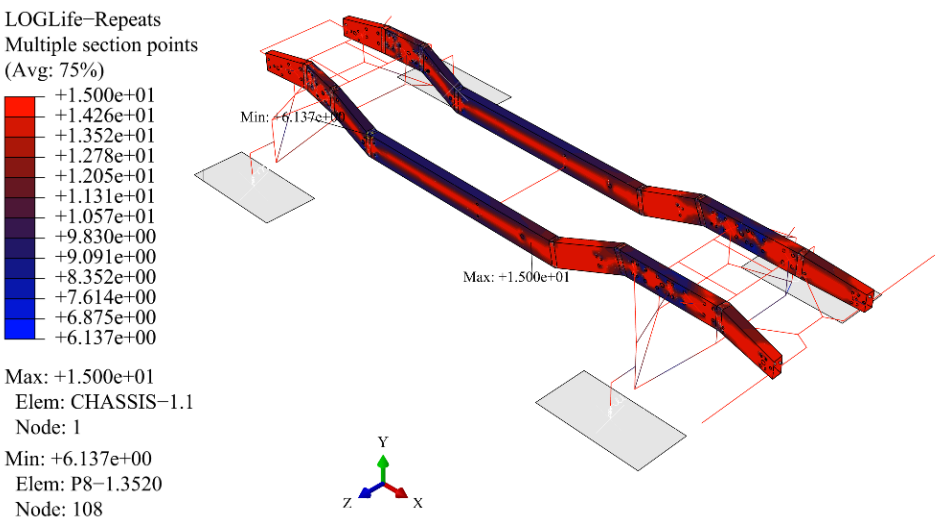

Received: 28.05.2021 – Accepted: 25.06.2021

(c)

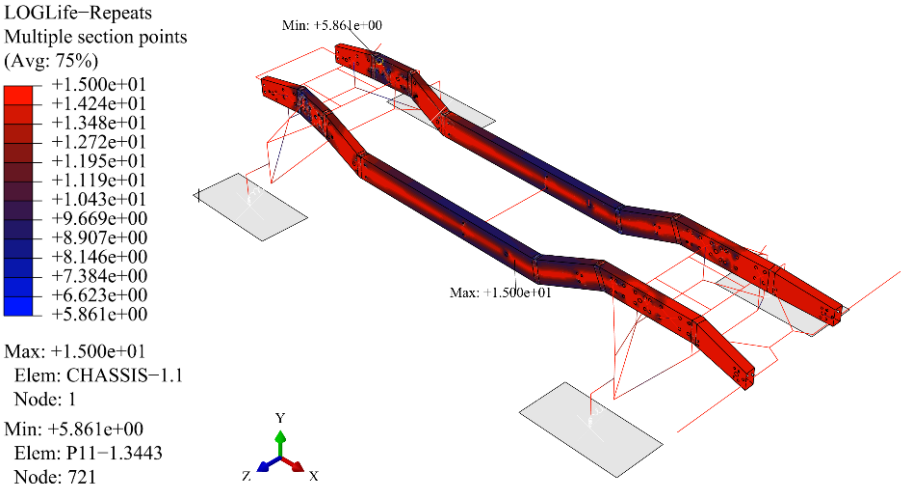

(d)

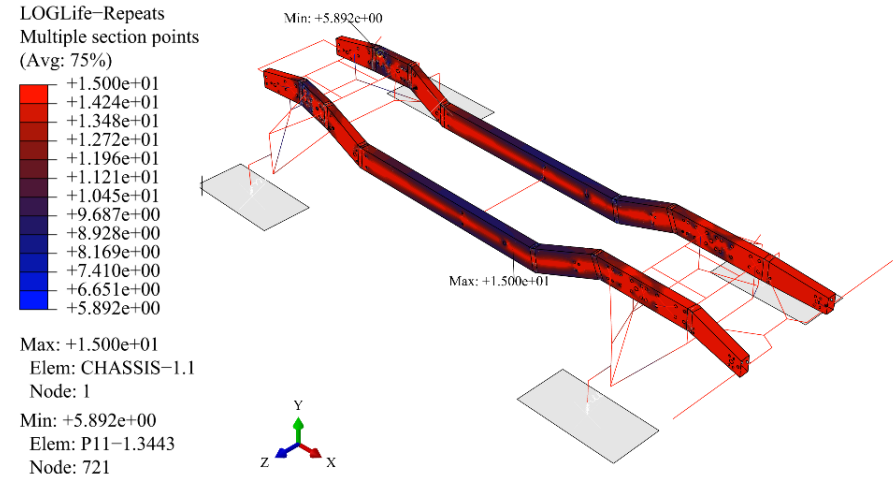

(e)

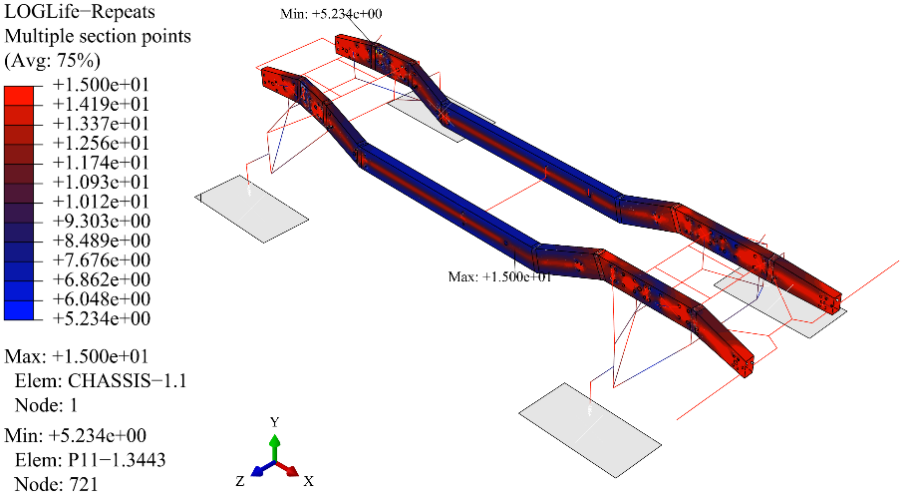

Received: 28.05.2021 – Accepted: 25.06.2021

(f)

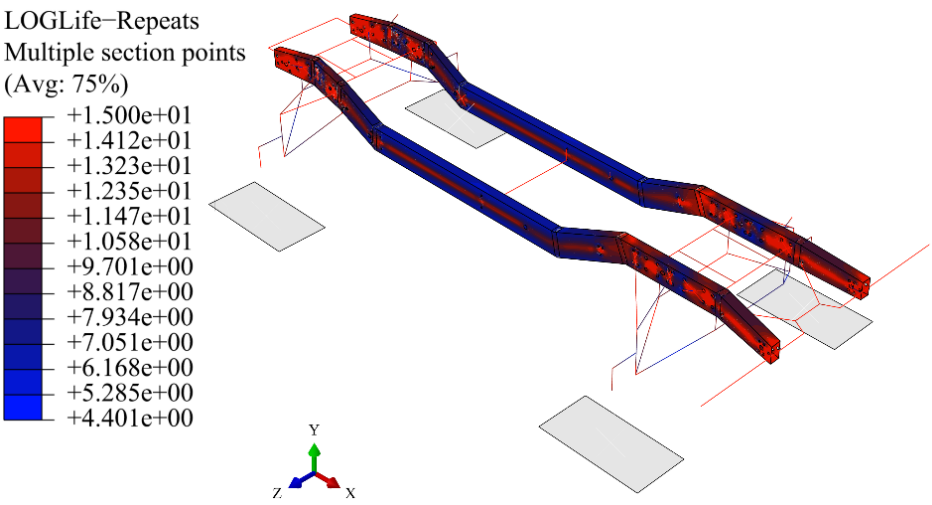
LOGLife−Repeats
Multiple section points
(Avg: 75%)
+1.500e+01
+1.412e+01
+1.323e+01
+1.235e+01
+1.147e+01
+1.058e+01
+9.701e+00
+8.817e+00
+7.934e+00
+7.051e+00
+6.168e+00
+5.285e+00
+4.401e+00
Y
Z
X

(g)

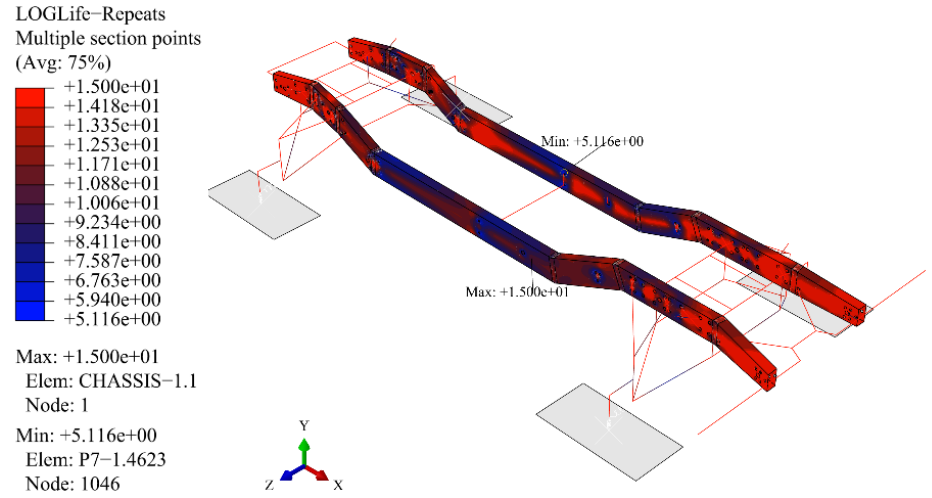
LOGLife−Repeats
Multiple section points
(Avg: 75%)
+1.500e+01
+1.418e+01
+1.335e+01
+1.253e+01
+1.171e+01
+1.088e+01
+1.006e+01
+9.234e+00
+8.411e+00
+7.587e+00
+6.763e+00
+5.940e+00
+5.116e+00
Max: +1.500e+01
Elem: CHASSIS−1.1
Node: 1
Min: +5.116e+00
Elem: P7−1.4623
Node: 1046
Min: +5.116e+00
Max: +1.500e+01
Y
Z
X

(h)

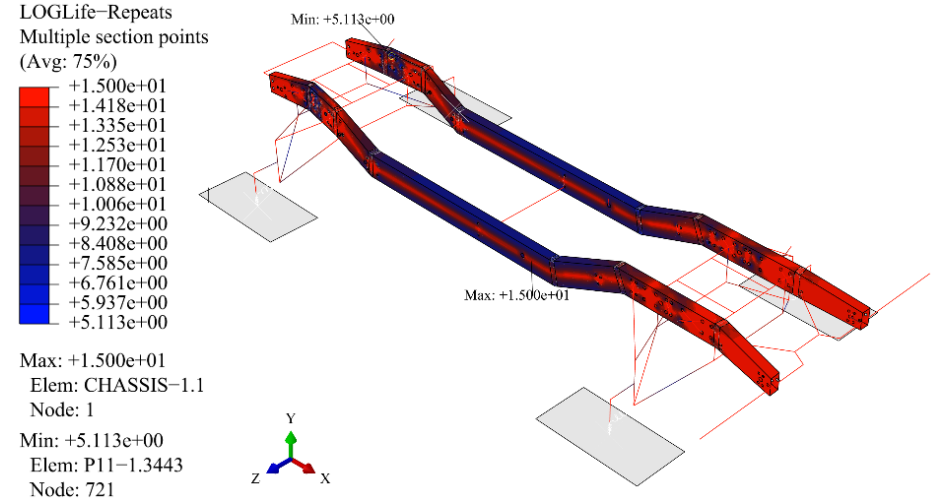
LOGLife−Repeats
Multiple section points
(Avg: 75%)
+1.500e+01
+1.418e+01
+1.335e+01
+1.253e+01
+1.170e+01
+1.088e+01
+1.006e+01
+9.232e+00
+8.408e+00
+7.585e+00
+6.761e+00
+5.937e+00
+5.113e+00
Max: +1.500e+01
Elem: CHASSIS−1.1
Node: 1
Min: +5.113e+00
Elem: P11−1.3443
Node: 721
Min: +5.113e+00
Max: +1.500e+01
Y
Z
X

4. Conclusion

In this article, stress analysis and fatigue life estimation of a car chassis are evaluated. The chassis experienced six major maneuvers including acceleration, deceleration, pothole, drop, sinusoidal obstacle, and turning. A new strategy for welding was considered in which a reinforcement plate attached under the 15 mm-gap joint between two adjacent profiles. Adding these plates will result in a 14 % reduction in maximum Von Mises stress. Stress analysis revealed that full acceleration with 168 MPa and 300 mm drop with 565 MPa have the lowest and highest Von Mises stress. Besides the stress analysis, fatigue life prediction has been evaluated with the help of FE-Safe software. 300 mm drop with 25000 cycle and Full acceleration with 1370000 cycles are the lowest and highest fatigue life cycle, respectively. The results of this study can be the focus of future studies in order to design more accurate geometry of welding profiles using different optimization method.

References

Ablat, M.A., & Qattawi, A. (2017). Numerical simulation of sheet metal forming: a review. *International Journal of Advanced Manufacturing Technology*, *89*(1–4), 1235–1250. https://doi.org/10.1007/s00170-016-9103-5

Abry, J., Mittelhaeuser, C., Wolf, S., & Turlier, D. (2018). Enhanced fatigue structural stress analysis of a heavy vehicle seam welded steel chassis frame: FEA model preparation, weld model description, fatigue stress calculation and correlation with 10 year operating experience. *Procedia Engineering*, *213*, 539–548. https://doi.org/10.1016/j.proeng.2018.02.050

Balaji, D.S., Prabhakaran, S., & Umanath, K. (2017). Design and analysis of the double wishbone suspension system. *Journal of Advanced Research in Dynamical and Control Systems*, *9*(2 Special Issue), 987–993.

Bhatnagar, U., Chaturvedi, P., & Gupta, A. (2018). Analysis and Proposed Fabrication of Four-Wheeler Chassis. *2018 International Conference on Automation and Computational Engineering, ICACE 2018*, 40–44. https://doi.org/10.1109/ICACE.2018.8686993

Chattopadhyay, A., Glinka, G., El-Zein, M., Qian, J., & Formas, R. (2011). Stress analysis and fatigue of welded structures. *Welding in the World*, *55*(7–8), 2–21. https://doi.org/10.1007/BF03321303

Deulgaonkar, V. R. (2019). *Finite Element Analysis of Chassis Integrated Structure for Tractor Trolley in Agricultural Applications*. *11*(1), 4273. https://doi.org/10.4273/ijvss.11.1.13

Fricke, W. (2003). Fatigue analysis of welded joints: State of development. In *Marine Structures*, 16(3), 185–200. Elsevier BV. https://doi.org/10.1016/S0951-8339(02)00075-8

Gorash, Y., Comlekci, T., & Mackenzie, D. (2015). Comparative Study of FE-models and Material Data for Fatigue Life Assessments of Welded Thin-walled Cross-beam Connections. *Procedia Engineering*, *133*, 420–432. https://doi.org/10.1016/j.proeng.2015.12.612

Hazimi, H., Ubaidillah, Setiyawan, A.E.P., Ramdhani, H.C., Saputra, M.Z., & Imaduddin, F. (2018). Vertical bending strength and torsional rigidity analysis of formula student car chassis. *AIP Conference Proceedings*, *1931*(1), 030050. https://doi.org/10.1063/1.5024109

James L. Meriam, L.G. Kraige, J.N.B. (2015). *Engineering Mechanics: Dynamics* (8th ed.). Wiley.

Khatoon, S., & Kim, M.H. (2020). Thermal Comfort in the Passenger Compartment Using a 3-D Numerical Analysis and Comparison with Fanger's Comfort Models. *Energies*, *13*(3), 690. https://doi.org/10.3390/en13030690

Kim, Y., Oh, J.S., & Jeon, S.H. (2015). Novel hot spot stress calculations for welded joints using 3D solid finite elements. *Marine Structures*, *44*, 1–18. https://doi.org/10.1016/j.marstruc.2015.07.004

Kumar, L.R., Krishnan, A.V., Yashwant, K., & Aravindan, B. (2020). *Design and analysis of all terrain vehicle chassis using finite element analysis Design and Analysis of All Terrain Vehicle Chassis using Finite Element Analysis*. *020093*(October).

Meneghetti, G. (2008). The peak stress method applied to fatigue assessments of steel and aluminium fillet-welded joints subjected to mode I loading. *Fatigue & Fracture of Engineering Materials and Structures*, *31*(5), 346–369. https://doi.org/10.1111/j.1460-2695.2008.01230.x

Mohamad, M.L., Rahman, M.T.A., Khan, S.F., Basha, M.H., Adom, A.H., & Hashim, M.S.M. (2017). Design and static structural analysis of a race car chassis for Formula Society of Automotive Engineers (FSAE) event. *Journal of Physics: Conference Series*, *908*(1), 012042. https://doi.org/10.1088/1742-6596/908/1/012042

N, A.M., Nandu, N.C., Krishnan, A., Nair, A R., & Sreedharan, P. (2018). ScienceDirect Design , Analysis , Fabrication and Testing of a Formula Car Chassis. *Materials Today: Proceedings*, *5*(11), 24944–24953. https://doi.org/10.1016/j.matpr.2018.10.295

Oanta, E., Raicu, A., & Menabil, B. (2020). Applications of the numerical methods in mechanical engineering experimental studies. *IOP Conference Series: Materials Science and Engineering*, *916*(1). https://doi.org/10.1088/1757-899X/916/1/012074

Paraforos, D.S., Griepentrog, H.W., & Vougioukas, S.G. (2016). Country road and field surface profiles acquisition, modelling and synthetic realisation for evaluating fatigue life of agricultural machinery. *Journal of Terramechanics*, *63*, 1–12. https://doi.org/10.1016/j.jterra.2015.10.001

Podkowski, K., Stasiak, A., & Pawlak, M. (2019). *Testing of the Torsional Stiffness of the Passenger Car Frame and its Validation by Means*. *85*(3), 83–101.

Ren, Y., Yu, Y., Zhao, B., Fan, C., & Li, H. (2017). *Finite Element Analysis and Optimal Design for the Frame of SX360 Dump Trucks*. *174*, 638–647. https://doi.org/10.1016/j.proeng.2017.01.201

Sankar, S.L., Arunkumar, G., & Suresh, A.V. (2018). Design and analysis of wishbones in double wishbone suspension system: Technical Note. *International Journal of Vehicle Structures and Systems*, *10*(4), 260–262. https://doi.org/10.4273/ijvss.10.4.06

Sharma, V., Reddy, D.M., & Patil, S. (2021). Stress Analysis of Automotive Chassis Using Hypermesh and Optistruct. *Lecture Notes in Mechanical Engineering*, 169–185. https://doi.org/10.1007/978-981-15-5947-1_14

Str, C.D., Tu, B., & Dist, L. (2019). *Finite Element Analysis in Automobile Chassis Design Nguyen Thanh Quang *. 889*, 461–468. https://doi.org/10.4028/www.scientific.net/AMM.889.461

Tsirogiannis, E.C., Stavroulakis, G.E., & Makridis, S.S. (2019). Electric Car Chassis for Shell Eco Marathon Competition: Design, Modelling and Finite Element Analysis. *World Electric Vehicle Journal*, *10*(1), 8. https://doi.org/10.3390/wevj10010008

Wang, P., Nai, M.L.S., Sin, W.J., Lu, S., Zhang, B., Bai, J., Song, J., & Wei, J. (2018). Realizing a full volume component by in-situ welding during electron beam melting process. *Additive Manufacturing*, *22*, 375–380. https://doi.org/10.1016/j.addma.2018.05.022

Wang, Y., Yu, B., Berto, F., Cai, W., & Bao, K. (2019). Modern numerical methods and their applications in mechanical engineering. *Advances in Mechanical Engineering*, *11*(11), 168781401988725. https://doi.org/10.1177/1687814019887255

Wongchai, B. (2020). *Front and Side impact Analysis of Space Frame Chassis of Formula Car*. *18*(67), 168–174.

Zaidie, M.N.A., Hashim, M.S.M., Tasyrif, M., Basha, M.H., Ibrahim, I., Kamaruddin, N.S., & Shahriman, A.B. (2017). Analysis of a front suspension system for UniART FSAE car using FEA. *Journal of Physics: Conference Series*, *908*(1), 012058. https://doi.org/10.1088/1742-6596/908/1/012058